

Interstellar isotope ratios from mm-wave molecular absorption spectra

R. Lucas¹ and H. Liszt²

¹ Institut de Radioastronomie Millimétrique, 300 Rue de la Piscine, F-38406 Saint Martin d'Hères, France

² National Radio Astronomy Observatory, 520 Edgemont Road, Charlottesville, VA 22903-2475, USA

Received 18 March 1998 / Accepted 22 June 1998

Abstract. We have measured galactic $\lambda 3\text{mm}$ absorption spectra of HCO^+ , HCN , HNC , and CS toward compact extragalactic continuum sources in order to derive the isotopic abundance ratios $^{12}\text{C}/^{13}\text{C}$, $^{14}\text{N}/^{15}\text{N}$, $^{16}\text{O}/^{18}\text{O}$, and $^{32}\text{S}/^{34}\text{S}$ in local diffuse clouds. For carbon, our data confirm recent results for the local ISM: we find $^{12}\text{C}/^{13}\text{C} = 59 \pm 2$. For nitrogen, we find $^{14}\text{N}/^{15}\text{N} = 237(-21, +27)$ consistent with the Solar value of 270, but substantially smaller than the values inferred from HCN emission in dense clouds. For sulfur we find $^{32}\text{S}/^{34}\text{S} \approx 19 \pm 8$ consistent with the Solar value of 23. We also find one striking individual anomaly: toward 3C111 (B0415+379), $\text{H}^{12}\text{CN}/\text{H}^{13}\text{CN} = 170 \pm 50$ in one kinematic component. We attribute this to the fractionation of ^{13}C into ^{13}CO which may be so great that HCN is starved for ^{13}C .

Key words: ISM: abundances – ISM: clouds – ISM: molecules – ISM: structure – radio lines: interstellar

1. Introduction

Much of our knowledge of CNO isotope ratios in the local interstellar medium is derived from optical and mm-wave spectra of common molecules like CH , CH^+ , CO , CS , CN , HCN , *etc.* Of these, CH^+ is particularly important for sampling the diffuse gas because it is believed to be free of the chemical and other effects which might cause its $^{12}\text{C}/^{13}\text{C}$ ratio to differ from the intrinsic ISM value. CO , on the other hand, is useless in diffuse clouds, given its susceptibility to fractionation (Watson et al. 1976) and selective photodissociation (Van Dishoeck & Black 1988; Kopp et al. 1996). But it is the most accurate probe of the densest clouds if problems with line saturation can be overcome by observing the rarest isotopomers (Langer et al. 1984).

The most recent values of $^{12}\text{C}/^{13}\text{C}$ measured in CH^+ toward ζ Oph are 67.6 ± 4.5 from Crane et al. (1991), 68 ± 7 from Stahl & Wilson (1992), and 63 ± 8 from Hawkins et al. (1993), leading to $\langle ^{12}\text{C}/^{13}\text{C} \rangle = 67 \pm 4$. This agrees well with the value $\langle ^{12}\text{C}/^{13}\text{C} \rangle = 62 \pm 4$ derived by Langer & Penzias (1993) from C^{18}O and $^{13}\text{C}^{18}\text{O}$ emission profiles toward 4 local dense

clouds. Nonetheless, discrepant results abound. The $^{12}\text{C}/^{13}\text{C}$ ratio measured in CN absorption toward ζ Oph by Crane & Hegyi (1988) is $47.3(+5.5, -4.4)$ and $^{12}\text{C}/^{13}\text{C}$ ratios from the *uv* absorption of CO vary so widely that even the effects of fractionation, *etc.* cannot be gauged: $^{12}\text{C}/^{13}\text{C} = 55$ from Wannier et al. (1991), 82 from Lyu et al. (1994) and 167 from Lambert et al. (1994).

For dense clouds observed in emission at mm-wavelengths, species not chemically related to CO are expected to have $^{12}\text{C}/^{13}\text{C}$ ratios higher than that in the gas generally, owing to fractionation reactions (Langer et al. 1984). If $\text{C}/\text{O} < 1$, the $^{12}\text{C}/^{13}\text{C}$ ratio in CO should have very nearly the correct, intrinsic value (because nearly all the ^{12}C is in ^{12}CO) but H_2CO and HCN are somewhat starved for ^{13}C and their isotopomers carry a $^{12}\text{C}/^{13}\text{C}$ ratio which is too large. If $\text{C}/\text{O} > 1$, the $^{12}\text{C}/^{13}\text{C}$ ratio measured in CO should be smaller than the intrinsic value, but only negligibly so at high enough density. In this case the ratios in HCN , *etc.* are above the intrinsic value and diverge increasingly from it even as the ratio in CO becomes more reliable. In general, the intrinsic $^{12}\text{C}/^{13}\text{C}$ ratio is bounded below by the ratios seen in CO and above by those in H_2CO , *etc.*, but the former should be much closer to the true value.

For nitrogen, most information about the $^{14}\text{N}/^{15}\text{N}$ ratio comes from measurements of HCN emission (Wannier et al. 1981; Wilson & Rood 1994; Dahmen et al. 1995). Because $\text{H}^{12}\text{C}^{14}\text{N}$ emission is so optically thick, only the so-called double ratio $\text{H}^{13}\text{CN}/\text{HC}^{15}\text{N} = (\text{H}^{13}\text{CN}/\text{H}^{12}\text{C}^{14}\text{N}) \times (\text{H}^{12}\text{C}^{14}\text{N}/\text{H}^{12}\text{C}^{15}\text{N})$ can be measured. But the $^{12}\text{C}/^{13}\text{C}$ ratio in HCN differs from that in the gas at large depending on fractionation and cloud properties in a degree which can only be estimated from observations of similarly-affected species like H_2CO . Indeed, the $^{12}\text{C}/^{13}\text{C}$ ratios derived from H_2CO are uniformly larger than those found from CO (see Fig. 2 of Wilson & Rood (1994), but note their errors of labelling). This sensitivity to physical conditions opens the possibility that gradients in cloud structure across the galactic disk could be wrongly interpreted as variations in the nitrogen and carbon isotope ratios.

Here, we try a new approach to the measurement of CNO and sulfur isotope ratios in the local ISM based on the study of mm-wave molecular absorption profiles. Somewhat surprisingly, the abundances of many polyatomic species are quite high in rather diffuse regions where the extinction is not large, with

Send offprint requests to: R. Lucas

Correspondence to: lucas@iram.fr

Table 1. Background sources observed in HCO^+

Source	Alias	l °	b °	$\sigma_{l/c}$ H^{12}CO^+	$\sigma_{l/c}$ H^{13}CO^+
B0355+508	NRAO150	150.4	-1.6	0.0180	0.0170
B0415+379 ^a	3C111	161.7	-8.8	0.0023	0.0036
B0528+134		191.4	-11.0	0.0120	0.0160
B1730-130	NRAO530	12.0	10.8	0.0210	0.0042

^a $\sigma_{l/c} = 0.0029$ for HC^{18}O^+ **Table 2.** RMS noise $\sigma_{l/c}$ for HCN, HNC, and CS ($J=2-1$)

Source	H^{12}CN	H^{13}CN	HN^{12}C	HN^{13}C	C^{32}S	C^{34}S
B0355	0.022	0.027			0.044	0.017
B0415 ^a	0.044	0.003	0.0044	0.0033	0.030	0.025

^a for HC^{15}N $\sigma_{l/c} = 0.0036$

$N(\text{HCO}^+) \approx 1 - 2 \times 10^{12} \text{ cm}^{-2}$, $N(\text{OH}) \approx 4 - 8 \times 10^{13} \text{ cm}^{-2}$, $N(\text{CO}) \approx 3 - 10 \times 10^{15} \text{ cm}^{-2}$ (Lucas & Liszt 1993, 1994, 1996, 1997; Liszt & Lucas 1994, 1996, 1998; Hogerheijde et al. 1995) at $N(\text{H}_2) \approx 5 \times 10^{20} \text{ cm}^{-2}$ (Lucas & Liszt 1996). In many of these clouds, lines of the most abundant isotope of such common species as HCO^+ , HCN, HNC, CS, *etc.* are strong but not saturated and rotational excitation is demonstrably insignificant (Lucas & Liszt 1996). Given these two conditions, there is no need to resort to measurement of double ratios involving more than one isotopic substitution. Thus the total column density may be reliably and straightforwardly derived from observations of even a single transition.

This investigation is also helped by several circumstances regarding the chemistry. The species studied here are not known to be affected by selective photodissociation and are not directly fractionated by reactions with C^+ , the dominant form of carbon. Except perhaps for HCO^+ , they are also not fractionated indirectly in molecule-molecule reactions. The abundance of CO is typically small and fractionation effects stemming from loss of the ambient carbon reservoir to CO are minimized. The diffuse character of the gas means that depletion and gas-grain interactions are also reduced in importance.

In Sect. 2 we describe the new observations of mm-wave molecular absorption which we have made. In Sect. 3 we derive isotope ratios and compare our results with previous determinations. In Sect. 4 we discuss the anomalous $\text{H}^{12}\text{CN}/\text{H}^{13}\text{CN}$ ratio seen in one kinematic component toward B0415+379 in Taurus. In the following, we do not explicitly give the atomic weight of the normal isotope.

2. Our data

2.1. Absorption line profiles

The absorption observations discussed here were taken at the Plateau de Bure Interferometer (Guilloteau et al. 1992) during the 1993-1997 observing seasons and have been treated in a manner similar to that discussed in Lucas & Liszt (1996, LL96).

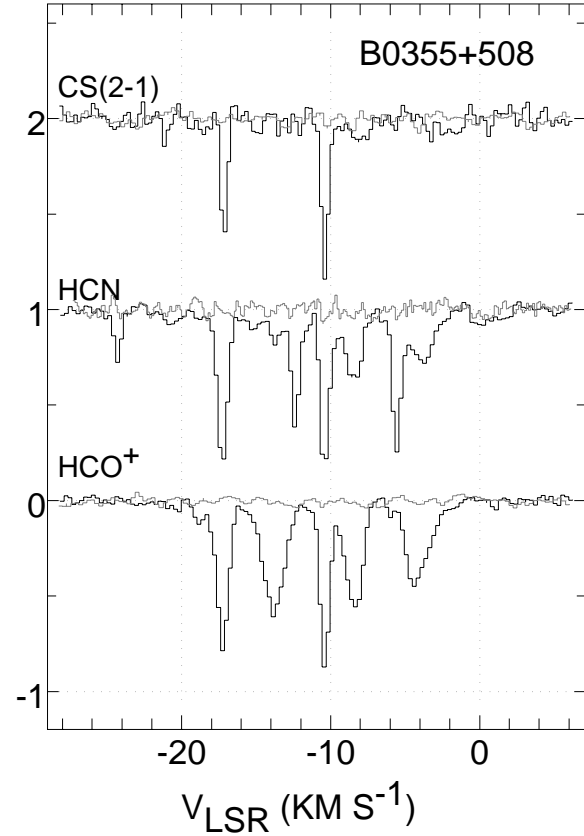


Fig. 1. H^{12}CO^+ , H^{12}CN , and C^{32}S ($J=2-1$) absorption spectra toward B0355+508=NRAO150 (solid lines) with H^{13}CO^+ , H^{13}CN , and C^{34}S overlaid (shaded).

The spectra have a channel spacing of 78.1 kHz, corresponding to 0.264, 0.263, 0.258, and 0.239 km s^{-1} for the main isotopes of HCN, HCO^+ , HNC, and CS ($J=2-1$), respectively. The resolution of the spectrometer, however, is only 140 kHz.

The absorption line source list is summarized in Table 1 where we give 1) B1950 source name; 2) any alias; 3-4) galactic coordinates; 5-6) $\sigma_{l/c}$, the channel-to-channel rms for the line/continuum flux ratio (the rms optical depth noise at zero optical depth) for the H^{12}CO^+ and H^{13}CO^+ $J=1-0$ line profiles. Since the background sources are time-variable we have made weighted averages of the line/continuum ratio over several observing sessions. In Table 2 we show the noise levels reached for those sources in which species beside HCO^+ were observed. The high signal/noise ratios attained toward B0415+379 and B1730-130 result from the fortuitously high fluxes of these sources, $\approx 10\text{Jy}$, at certain times during our work.

The spectra are shown in Figs. 1-3 where the various isotopes of the various species are superposed, with the weakest ones shaded and occasionally scaled as indicated in the figure captions. Column densities derived from these spectra are given in Tables 3-6. In many cases we have not attempted to derive isotope ratios for individual features either because there is inadequate signal/noise or because the components overlap so substantially; such is the case for the HCO^+ observed toward B0355+508 and B0415+379, respectively. The CS column den-

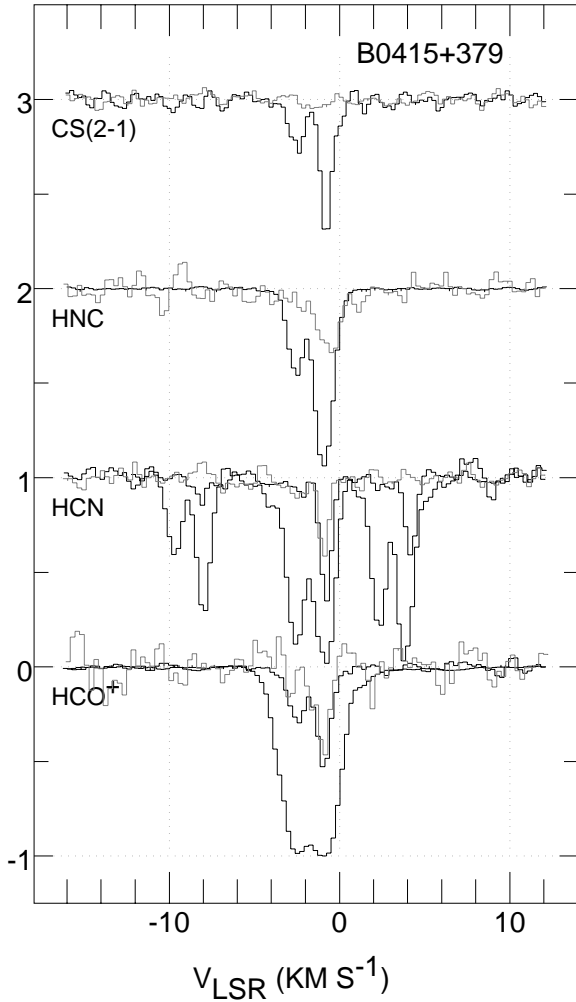


Fig. 2. $\text{H}^{12}\text{C}^{16}\text{O}^+$, H^{13}CO^+ ($\times 5$), $\text{H}^{12}\text{C}^{14}\text{N}$, $\text{H}^{13}\text{C}^{14}\text{N}$ ($\times 7$), $\text{H}^{14}\text{N}^{12}\text{C}$, and $^{12}\text{C}^{32}\text{S}$ ($J=2-1$) absorption spectra toward B0415+379=3C111 (solid lines) with $\text{H}^{12}\text{C}^{18}\text{O}^+$ ($\times 27.5$), $\text{H}^{12}\text{C}^{15}\text{N}$ ($\times 10$), $\text{H}^{14}\text{N}^{13}\text{C}$ ($\times 15$) and C^{34}S overlaid (shaded).

sities in two clouds toward this source arise from integration over the profile (Table 6). In Tables 4 and 6 all values for individual components arise from fitting Gaussian components to the absorption profiles $1 - \exp(-\tau(v))$; the results of integrating over the entire profile, which gives a somewhat lower nominal total HCN column density, are listed separately. Toward B0415+379 the H^{12}CO^+ is optically thick enough that a unique decomposition of the profile is impossible even though the line integral is quite well constrained by the available 435:1 peak signal/noise ratio. For very thick lines, proper error estimates for the peak optical depth and profile integral become increasingly asymmetrical and larger on the side of higher optical depth. Where necessary we derived error estimates from a Monte Carlo simulation using the observed profile and empirically measured noise in the line/continuum ratio, as given in Tables 1 and 2.

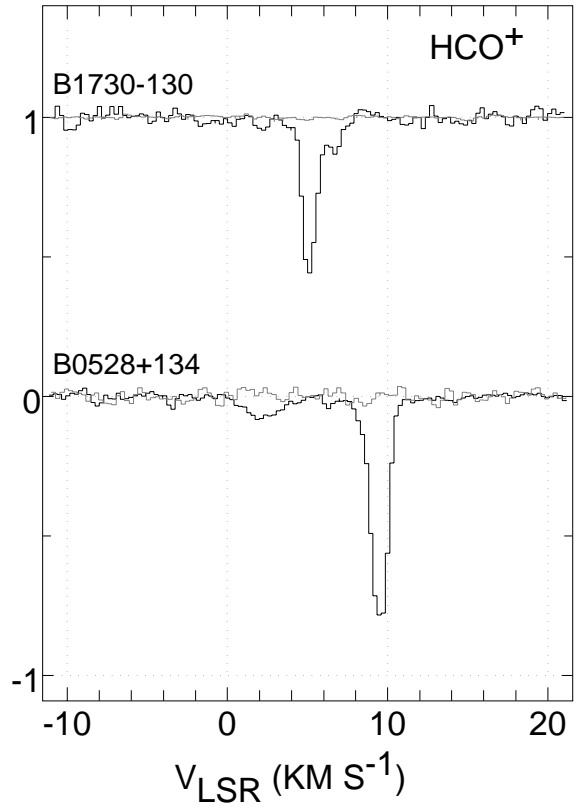


Fig. 3. H^{12}CO^+ (solid lines) and H^{13}CO^+ (overlaid, shaded) absorption spectra toward B0528+134 and B1730-130 (NRAO530).

Table 3. $^{12}\text{C}/^{13}\text{C}$ derived from observations of HCO^+

Source	$N(\text{H}^{12}\text{CO}^+)$ 10^{12} cm^{-2}	$N(\text{H}^{13}\text{CO}^+)$ 10^{11} cm^{-2}	$^{12}\text{C}/^{13}\text{C}$
B0355+508	6.08(0.07)	1.12(0.35)	54 (17)
B0415+379 ^a	12.9(-0.4, +1.0)	2.11 (0.05)	61 (-3, +5)
B0528+134	1.82 (0.03)	< 0.40 ^b	> 45 ^b
B1730-130	0.94 (0.03)	0.196 (0.055)	48 (14)

^a $N(\text{HC}^{18}\text{O}^+) = 1.92(0.28) \times 10^{10} \text{ cm}^{-2}$

^b 2σ

2.2. Common conventions

All velocities quoted here are measured with respect to the Local Standard of Rest. All limits are twice the empirically-determined rms. Unless otherwise stated the $J=1-0$ line and the most abundant isotope are intended.

3. Column densities and isotopic abundance ratios

The basic equation needed here is the relationship between the column densities N_J in rotation levels J , and the optical depths $\tau_{J,J+1}$ of the rotational transitions $J \rightarrow J+1$, for linear rotors like the species studied here:

$$N_J = \frac{(2J+1)}{(J+1)} \frac{8.0 \times 10^{12} \text{ cm}^{-2} \int \tau_{J,J+1} dv}{\mu^2 (1 - \exp(-h\nu/kT_{\text{ex}}))}$$

Table 4. $^{12}\text{C}/^{13}\text{C}$ and $^{14}\text{N}/^{15}\text{N}$ derived from observations of HCN

Source	v km s^{-1}	$N(\text{H}^{12}\text{C}^{14}\text{N})$ 10^{12} cm^{-2}	$N(\text{H}^{13}\text{CN})$ 10^{11} cm^{-2}	$N(\text{HC}^{15}\text{N})$ 10^{10} cm^{-2}	$^{12}\text{C}/^{13}\text{C}$	$^{14}\text{N}/^{15}\text{N}$
B0355+508		10.7(.20)	$< 1.9^a$		> 58	
B0415+379 ^b	-2.5	8.50(0.27)	0.50(0.15)	3.48 (1.27)	170 (51)	244 (89)
	-0.9	15.9(0.40)	2.73(0.10)	5.62 (0.73)	58 (3)	282 (37)
B0415+379 ^c	all	21.7 (-0.4, +2.6)	3.31 (0.18)	9.14 (0.79)	66 (-4, +9)	237 (-21, +27)

^a 2σ ^b from Gaussian decomposition^c from profile integral

where μ is the permanent dipole moment in Debye, 10^{-18} esu ($\mu = 0.11\text{D}$ for CO, 4.07D for HCO^+ , 3.05D for HNC, and 2.98D for HCN), the integrated optical depth is in units of km s^{-1} , and T_{ex} is the excitation temperature between levels J and $J + 1$. As mentioned in the Introduction (see Lucas & Liszt 1996) the excitation temperatures of the levels studied here do not differ appreciably from that of the 2.7 K background.

3.1. The $^{12}\text{C}/^{13}\text{C}$ ratio

Carbon isotope ratios are available from HCO^+ , HCN, and HNC (Tables 3–5). With one rather stunning exception which we discuss at length in Sect. 4 (the lack of H^{13}CN at $v = -2.5 \text{ km s}^{-1}$ toward B0415+379), the results are quite consistent, although the data toward 3C111 contributes most strongly to the final result. The result of taking a weighted average of the six components in which the ^{13}C isotope was detected above the 2σ level, neglecting the anomaly toward 3C111, is $[^{12}\text{C}]/[^{13}\text{C}] = 59 \pm 2$. This is largely the average over several species in two nearby clouds toward 3C111, though the data in other directions are entirely consistent with it. Our data suggest that this sort of mm-wave interferometer absorption measurement will, in the future, be capable of discerning even very subtle cloud-to-cloud variations in the isotope ratio.

3.2. The $^{14}\text{N}/^{15}\text{N}$ ratio

This ratio is available only toward B0415+379 (Table 4). The results for both clouds are quite consistent and the sum over the profile suggests a possible slight enhancement of ^{15}N relative to the Solar System ratio of 270. The two clouds seen toward 3C111 are probably separated by about 200 pc along the line of sight, as discussed in Sect. 4.

Our results are at the very low end of the range of extant results based on HCN emission (Wannier et al. 1981; Wilson & Rood 1994; Dahmen et al. 1995) which yield a mean value $< ^{14}\text{N}/^{15}\text{N} > \approx 400$ for the nearby ISM if the $\text{H}^{12}\text{CN}/\text{H}^{13}\text{CN}$ ratio is 75–80. The nitrogen isotope ratios derived from NH_3 by Güsten & Ungerechts (1985) are 440–450 for DR21(OH) and S140, and 300–360 for W3(OH).

Table 5. $^{12}\text{C}/^{13}\text{C}$ derived from observations of HNC

Source	$N(\text{HN}^{12}\text{C})$ 10^{12} cm^{-2}	$N(\text{HN}^{13}\text{C})$ 10^{10} cm^{-2}	$^{12}\text{C}/^{13}\text{C}$
B0415+379	6.01 (0.04)	9.69 (0.89)	62 (6)

Table 6. $^{32}\text{S}/^{34}\text{S}$ derived from observations of $\text{CS}(J=2-1)^a$

Source	v km s^{-1}	$N(\text{C}^{32}\text{S})$ 10^{12} cm^{-2}	$N(\text{C}^{34}\text{S})$ 10^{11} cm^{-2}	$^{32}\text{S}/^{34}\text{S}$
B0355+508	-17.2	4.67(0.52)	< 3.2	> 15
	-10.3	9.66(0.98)	< 4.4	> 22
B0415+379	-2.5	3.96(0.51)	< 4.6	> 9
	-0.9	10.18(0.71)	5.98(2.30)	17(7)
	all	15.18(0.58)	0.79(0.31)	19(8)

^a all limits are 2σ

3.3. The $^{32}\text{S}/^{34}\text{S}$ ratio

This ratio was measured in two sources (Table 6) but the results are not as statistically significant as for carbon or nitrogen. Our value for the sulfur isotope ratio $^{32}\text{S}/^{34}\text{S} = 19 \pm 8$ is consistent with the Solar System ratio of 22.7, as seen earlier by Frerking et al. (1980).

3.4. The $^{16}\text{O}/^{18}\text{O}$ ratio

This ratio was measured in HCO^+ only one source (see the footnote to Table 3 and Fig. 2 at bottom) and seems to be the first determination not employing a double ratio involving two isotopic substitutions. Decomposition of the H^{13}CO^+ profile shows that about one-third of the total column density is in the component at -0.9 km s^{-1} , while nearly 60% is in the component at -2.5 km s^{-1} . The HC^{18}O^+ profile appears to show the lower-velocity line only rather weakly. We attribute the appearance of the HC^{18}O^+ to noise since several spurious features strong enough to affect the weaker line are clearly visible in adjacent regions of the passband.

Carbon/oxygen and oxygen isotope ratios for the integrated profiles are $^{13}\text{C}/^{18}\text{O} = 11 \pm 2$ and $^{16}\text{O}/^{18}\text{O} \simeq 672 \pm 110$ (the actual error is somewhat asymmetrically distributed, see Table 3). The $^{16}\text{O}/^{18}\text{O}$ ratio is consistent with the local ISM value 560 ± 25 based on H_2CO data (Wilson & Rood 1994), if not with the Solar System value of 489.

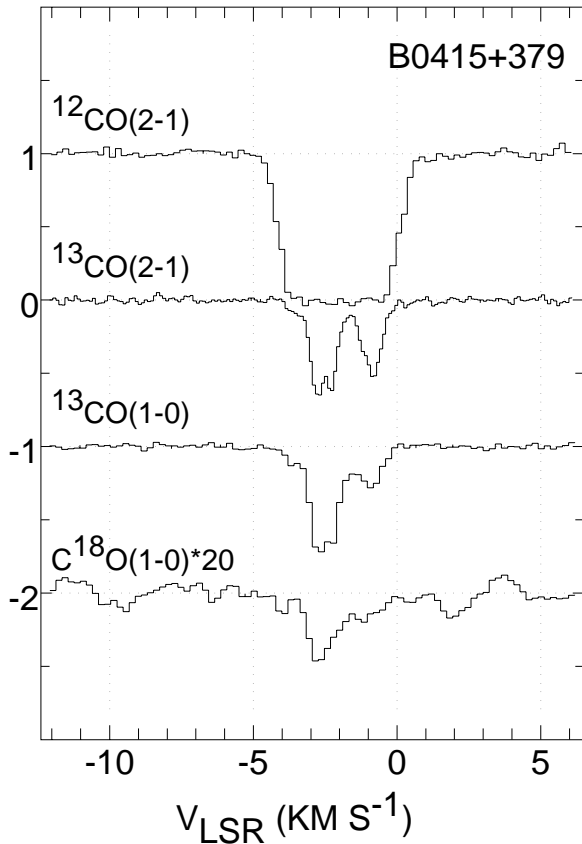


Fig. 4. CO absorption spectra toward B041+379, scaled as noted.

4. Discussion

4.1. CO fractionation and anomalies in molecular isotope ratios

In order to have any confidence in our isotope ratios, it is necessary to explain the evident lack of H^{13}CN in the -2.5 km s^{-1} cloud toward B0415+379. All three hyperfine components of the rarer isotope show the same effect, so this is not a spurious result arising from an unrecognized problem with one profile. Conversely, the H^{12}CN profiles, although somewhat saturated in the main line, have optically thin hyperfine components which allow an accurate column density measurement. H^{13}CO^+ is clearly present at -2.5 km s^{-1} but the signal/noise ratio in the HN^{13}C profiles is not high enough to make conclusive statements about the carbon isotopic abundance ratio.

In the Introduction we discussed the effect of fractionation in dense clouds where the carbon isotope ratio in CO is little affected: this is the usual explanation of the comparatively high $^{12}\text{C}/^{13}\text{C}$ ratios seen in H_2CO and inferred for HCN (Wilson & Rood 1994). But it is implicit in the work of Watson et al. (1976) that fractionation of ^{13}C into ^{12}CO could also be strong enough to starve other species of ^{13}C even when $^{12}\text{CO}/^{12}\text{C}^+ < 1$ and $^{12}\text{CO}/^{13}\text{CO} \ll 60$. A prominent example of a prospective victim of such an effect is HCN, which is formed and destroyed in chemical reactions rather removed from CO. On the other hand, HCO^+ may receive ^{13}C from CO *via* the reaction $\text{H}_3^+ + ^{13}\text{CO}$

$\rightarrow \text{H}^{13}\text{CO}^+ + \text{H}_2$ and its ^{13}C isotope might be replenished in this way. One interesting aspect of this scheme is that it requires an effective H_3^+ chemistry in an environment where ^{13}C fractionation in CO is on-going, which implies a high abundance of both C^+ and electrons: $N(^{12}\text{C}^+) > N(^{12}\text{CO})$ for strong fractionation to occur.

Watson et al. (1976) also suggested that fractionation of ^{13}C into CO would affect other molecules in a time-dependent manner, as follows. Initially, other species are formed from a gas in which free ^{13}C is somewhat lacking and simple conservation of nuclei demands that their $^{12}\text{C}/^{13}\text{C}$ ratio be larger than the true cosmic value. In general, there is no known way to fractionate carbon directly in species beside CO because they either react chemically and very exothermically with C^+ or not at all. But if depletion onto grains is important, the fact that CO should be relatively slow to freeze out means that the carbon which is lost from the gas is ^{13}C -poor. Eventually, the $^{12}\text{C}/^{13}\text{C}$ ratio in the gas will decline and the $^{12}\text{C}/^{13}\text{C}$ values in all molecules will be below the initial value in the gas, with CO showing the most extreme departures.

A simulation of this effect Liszt (1978) found that the carbon abundance in the gas could decline precipitously and little effect on the isotope ratios was seen. Because the coldest, darkest regions, where depletion is strong and the temperature is low, are regions in which essentially all the gas phase carbon is in CO, little fractionation of CO actually occurs there. Because the clouds we have observed here have relatively small CO column densities, with visual extinction below 1 mag Liszt & Lucas (1998), the main effect of ^{13}C fractionation on other species must be the more direct one of simple isotope sequestration and starvation.

In order to explain the HCN data in this way, it must be the case that ^{13}CO is greatly enhanced at the same time that H^{13}CN is missing. In fact, unlike the other species seen toward B0415+379, $N(^{13}\text{CO})$ is larger in the lower-velocity gas: this is apparent from the CO absorption profiles shown in Fig. 4, taken from Liszt & Lucas (1998). From those spectra it is seen that both $N(^{13}\text{CO})$ and $N(\text{C}^{18}\text{O})$ are larger in the lower-velocity feature while the $J=1-0$ excitation temperature is greater in the other: the -0.9 km s^{-1} line is stronger in ^{12}CO and ^{13}CO emission (Liszt 1994).

The two features have $N(^{13}\text{CO}) = 2.3 \times 10^{15} \text{ cm}^{-2}$ and $0.9 \times 10^{15} \text{ cm}^{-2}$, based on a comparison of CO emission and absorption profiles, so that the ratio of ^{13}CO column densities in the two features is approximately reversed compared to HCO^+ , HCN, CS, *etc.* From $N(^{13}\text{CO})$ we can derive lower limits to the column density of H_2 , since $N(^{13}\text{CO})/N(\text{H}_2) \lesssim ([\text{C}]/[\text{H}])(^{12}\text{C}/^{13}\text{C}) = 2 \times 10^{-4}/59$. These are $6.9 \times 10^{20} \text{ H}_2 \text{ cm}^{-2}$ and $2.7 \times 10^{20} \text{ H}_2 \text{ cm}^{-2}$ for the two major clouds toward B0415+379. If all of the available ^{13}C in the lower-velocity cloud is in ^{13}CO , $A_V \approx 0.75 \text{ mag}$; for the other, we have only that $A_V > 0.3 \text{ mag}$.

The ratios of $J=1-0$ optical depths in the ^{13}CO and C^{18}O lines are 40 and 24 for the clouds at -2.5 and -0.9 km s^{-1} , respectively, which are typical of the CO data gathered by Liszt & Lucas (1998). While the ‘fractionation/starvation’ scheme

might be more attractive if an even greater enhancement of the $^{13}\text{CO}/^{18}\text{O}$ ratio were evident in the lower-velocity gas, or if it were not evident that the column density of CO overall is higher in that cloud, this is not expected. In general, the degree of fractionation increases with the overall CO abundance because self-shielding must be effective before fractionation can compete successfully against photodissociation (Liszt & Lucas 1998).

A conclusive test of this suggestion would be a sensitive spectrum of some species beside HCN showing a deficit of ^{13}C in the lower-velocity gas. This will be possible if B0415+379 flares again, or if some instrument with a much larger collecting area becomes available.

4.2. Conditions in the molecular gas toward 3C111

3C111 sits in the Taurus region in Cloud 12 of Ungerechts & Thaddeus (1987, UT87) which spans the objects L1443, L1459, L1478, NGC1579, and L1492 moving from West to East. Unfortunately the spatial or spectral resolution of UT87 was too low to discern the multiple nature of the lines (Figs 1–4 here; for CO emission see Liszt (1994) and LL98). At Cloud 12 peak 12d nearest 3C111 the mean velocity of their CO emission is -2.7 km s^{-1} , implying that the -0.9 km s^{-1} feature is weak.

Ungerer et al. (1985, U85) mapped C^{18}O emission near 3C111 but only the line at -2.5 km s^{-1} was seen, consistent with our CO profiles in absorption and emission. This suggests that either the extinction is higher or the uv radiation field is smaller in the -2.5 km s^{-1} gas, because of the well-known tendency of C^{18}O emission to turn on when $A_V = 1 - 2 \text{ mag}$ (U85, Fig. 7). C^{18}O emission directly toward 3C111 is very weak, however (LL98), and was not seen by U85. By contrast, the -0.9 km s^{-1} line has a higher excitation temperature and the weak HCO^+ emission around 3C111 occurs only at -1 km s^{-1} (LL96). This implies that the -0.9 km s^{-1} gas is denser, and it clearly has a preponderance of OH and HCO^+ seen in absorption.

The star count data of U85 near 3C111 show that the extinction increases abruptly from 0 to $0.85 \pm 0.15 \text{ mag}$ at $D = 150 \text{ pc}$, and again to $2.2 \pm 1 \text{ mag}$ at 380 pc ; toward 3C111, which sits in a small hole in the gas, $A_V \approx 1.3 \text{ mag}$, consistent with the near absence of C^{18}O emission. The first of these steps in A_V corresponds to the distance of the dark filaments in Taurus (see the discussion in UT87) and is generally associated with molecular emission at positive velocity. The gas at -2.5 km s^{-1} is considered to be the main molecular cloud and is always placed 350–380 pc from the Sun (U85, UT87), some 55 pc from the galactic plane. Locating the -0.9 km s^{-1} gas has not been an issue because it was neither detected in C^{18}O (U85) nor distinguished in ^{12}CO (UT87).

If the -0.9 km s^{-1} cloud is identified with the filaments at 140 pc, its extinction is $0.85 \pm 0.15 \text{ mag}$ and the inferred 0.75 mag extinction of the -2.5 km s^{-1} gas is marginally consistent with the claimed total of $A_V = 1.3 \text{ mag}$ derived from star counts. If both features arise in the same body at a distance of 380 pc, it seems hard to understand how they could share the small

gas column which remains after accounting for 0.85 mag in the supposedly unrelated foreground gas. The -0.9 km s^{-1} gas is apparent in emission (Liszt 1994 and LL98) and its contribution to determination of the total molecular gas mass was not missed. But this mass has heretofore been attributed to one cloud when there are two, and to the body whose density is lower, whose column density is probably lower toward 3C111, and whose chemistry is less well developed.

5. Summary

The $^{12}\text{C}/^{13}\text{C}$ isotope ratio 59 ± 2 derived from molecular absorption in this work agrees well with recent results from CH^+ (67 ± 4) and $\text{C}^{18}\text{O}/^{13}\text{C}^{18}\text{O}$ (62 ± 4). Our less precise result $^{16}\text{O}/^{18}\text{O} \approx 672 \pm 110$ is consistent with recently quoted results for the local ISM (560 ± 25) if not the Solar System value of 489. For sulfur we find $^{32}\text{S}/^{34}\text{S} = 19 \pm 8$, consistent with the Solar value of 22.7. Our value of the nitrogen isotopic abundance ratio $^{14}\text{N}/^{15}\text{N} = 237 (-21, +27)$ is at the very low end of the range of ratios derived in somewhat less direct fashion from HCN.

Our data show that strong chemical fractionation of ^{13}C into carbon monoxide may affect other species even when the abundance of ^{12}CO is relatively small, a phenomenon never observed before. In particular, we attribute the striking lack of H^{13}CN in one cloud toward 3C111, where $\text{H}^{12}\text{CN}/\text{H}^{13}\text{CN} = 170 \pm 50$, to this effect. The relative abundance of H^{13}CO^+ , although not unusual in that cloud, may nonetheless have also been strongly affected by the fractionation and subsequent exchange of ^{13}C with CO.

Acknowledgements. The National Radio Astronomy Observatory (NRAO) is operated by Associated Universities, Inc. under a cooperative agreement with the US National Science Foundation. We thank those other members of the IRAM (Grenoble) staff who diligently scheduled these time-consuming observations. The remarks of an anonymous referee were important in improving the presentation of this work.

References

- Crane, P. and Hegyi, D. J.: 1988, *ApJ* 326, L35
- Crane, P., Hegyi, D. J., and Lambert, D. L.: 1991, *ApJ* 378, 181
- Dahmen, G., Wilson, T. L., and Matteucci, F.: 1995, *A&A* 295, 194
- Frerking, M. A., Wilson, R. W., Linke, R. A., and Wannier, P. G.: 1980, *ApJ* 240, 65
- Guilloteau, S., Delannoy, J., Downes, D., Greve, A., Guelin, M., Lucas, R., Morris, D., Radford, S. J. E., Wink, J., Cernicharo, J., Forveille, T., Garcia-Burillo, S., Neri, R., Blondel, J., Perrigourad, A., Plathner, D., and Torres, M.: 1992, *A&A* 262, 624
- Güsten, R. and Ungerechts, H.: 1985, *A&A* 145, 241
- Hawkins, I., Craig, N., and Meyer, D. M.: 1993, *ApJ* 407, 185
- Hogerheijde, M. R., De Geus, E. J., Spaans, M., Van Langevelde, H. J., and Van Dishoeck, E. F.: 1995, *ApJ* 441, L93
- Kopp, M., Gerin, M., Roueff, E., and Le Boulbot, J.: 1996, *A&A* 305, 558
- Lambert, D. L., Sheffer, Y., Gilliland, R. L., and Federman, S. R.: 1994, *ApJ* 420, 756
- Langer, W. D., Graedel, T. E., Frerking, M. A., and Armentrout, P. B.: 1984, *ApJ* 277, 581

- Langer, W. D. and Penzias, A. A.: 1993, ApJ 408, 539
- Liszt, H. S.: 1978, ApJ 222, 484
- Liszt, H. S.: 1994, ApJ 429, 638
- Liszt, H. S. and Lucas, R.: 1994, ApJ 431, L131
- Liszt, H. S. and Lucas, R.: 1996, A&A 314, 917
- Liszt, H. S. and Lucas, R.: 1998, A&A, submitted (LL98)
- Lucas, R. and Liszt, H. S.: 1993, A&A 276, L33, (LL93)
- Lucas, R. and Liszt, H. S.: 1994, A&A 282, L5, (LL94)
- Lucas, R. and Liszt, H. S.: 1996, A&A 307, 237, (LL96)
- Lucas, R. and Liszt, H. S.: 1997, in D. J. Jansen, M. R. Hogerheijde, and E. F. Van Dishoeck (eds.), *Molecules in astrophysics: Probes and processes (IAU Symposium 178, held in Leiden, The Netherlands, July 1-5, 1996), Leiden: Kluwer*, p. 421, (LL97)
- Lyu, C.-H., Smith, A. M., and Bruhweiler, F. C.: 1994, ApJ 426, 254
- Stahl, O. and Wilson, T. L.: 1992, A&A 254, 327+
- Ungerechts, H. and Thaddeus, P.: 1987, ApJS 63, 645
- Ungerer, V., Nguyen-Quang-Rieu, Mauron, N., and Brillet, J.: 1985, A&A 146, 123
- Van Dishoeck, E. F. and Black, J. H.: 1988, ApJ 334, 771
- Wannier, P. G., Linke, R. A., and Penzias, A. A.: 1981, ApJ 247, 522
- Watson, W. D., Anicich, V. G., and Huntress, W. T., J.: 1976, ApJ 205, L165
- Wilson, T. L. and Rood, R.: 1994, ARA&A 32, 191